Optimal uses of reaction wheels in the pyramid configuration using a new minimum infinity-norm solution

Article *in* Aerospace Science and Technology · December 2014

DOI: 10.1016/j.ast.2014.09.002

CITATIONS
9

READS
770

3 authors:

Hyungjoo Yoon
Korea Aerospace Research Institute
29 PUBLICATIONS **707** CITATIONS
SEE PROFILE

Hyun Ho Seo
Korea Aerospace Research Institute
6 PUBLICATIONS **23** CITATIONS
SEE PROFILE

Hong-Taek Choi
Korea Aerospace Research Institute
9 PUBLICATIONS **44** CITATIONS
SEE PROFILE

Aerospace Science and Technology 39 (2014) 109–119

Contents lists available at ScienceDirect

Aerospace Science and Technology

www.elsevier.com/locate/aescte

Optimal uses of reaction wheels in the pyramid configuration using a new minimum infinity-norm solution

Hyungjoo Yoon *, Hyun Ho Seo, Hong-Taek Choi

Satellite Control System Department, Korea Aerospace Research Institute, Daejeon 305-806, Republic of Korea

ARTICLE INFO

Article history:
Received 2 May 2014
Received in revised form 30 July 2014
Accepted 6 September 2014
Available online 16 September 2014

Keywords:
Minimum infinity-norm solution
Time optimal maneuver
Reaction wheel array
Momentum envelope

ABSTRACT

In this study, simple methods are presented to improve the agility performance of a spacecraft with four reaction wheels in the pyramid configuration. A new and simple method is proposed to determine the momentum and the torque envelopes, which are defined as the maximum momentum and torque capacities of the wheel array, respectively. Then, based on the geometry of the envelopes, the best shape of the pyramid configuration needed to deliver optimal agility performance is discussed. In this paper, new methods are also proposed to optimally distribute three-dimensional torque and momentum commands, to the individual reaction wheels. The developed methods are based on the use of novel algorithms to solve minimum infinity-norm, or L_∞-norm, problems. These algorithms can easily be implemented with minimal modification of conventional ones, but yield considerable improvement of agility performance in numerical examples.

1. Introduction

Agility performance has become one of the key factors in developing/operating modern satellite systems, especially for Earth-imaging satellites, because it determines the number of available imaging targets within the duration of a given pass. Agility performance can be improved in various ways, but it is mainly determined by the maximum torque and momentum capacities of the actuators. A modern satellite is generally equipped with an array of at least three, possibly more, reaction wheels for redundancy. Hence, the total combined capacity of the array, which is referred to as an 'envelope', should be considered. This envelope is determined not only by the capacity of individual wheels, but also by the configuration of the wheel array. In this paper, we discuss how to determine the wheel configuration needed for optimal agility performance.

Another closely related problem that should be considered, is the efficient distribution of three-dimensional torque and momentum commands to individual reaction wheels. Because there are generally more than three reaction wheels, it becomes necessary to solve an under-determined linear-equations system, which in general has an infinite number of solutions.

In fact, this problem can be considered a special case of the control allocation problem. There have been a lot of investigations of control allocation problems for aircraft (see Ref. [7] and the references therein) and a few on spacecraft attitude control (e.g., see Ref. [3]). However, the focus of these studies was not the best use of wheel array capacity to achieve optimal agility, which is the main topic of this paper.

Conventionally, the minimum L_2-norm solution, which minimizes the square sum of the individual torque/momentum, is used because it minimizes the total power/energy of the wheel array. However, as will be shown later, this method does not fully utilize the envelopes of the wheel array. On the other hand, the minimum L_∞-norm (or 'infinity-norm') solution, which minimizes the maximum absolute value of the individual torque/momentum, may be a better choice for higher agility performance. While the minimum L_2-norm solution can easily be obtained using a pseudo-inverse matrix, it is well known that the minimum L_∞-norm solution cannot be expressed in a simple closed form, and thus needs more sophisticated algorithms to 'search' for it.

Cadzow proposed just such an algorithm [1,2]. His algorithm is efficient and is applicable to under-determined problems in any number of dimensions, but it is subject to the Haar condition [5]. Moreover, the algorithm does not solve the problem itself but, in fact, solves its 'dual optimization problem'. For this reason, it does not help much to understand the nature of the problem. Gravagne and Walker [4] proposed an algorithm also based on the dual problem, and showed how the solution could be applied to multi-link robot controls. Markley et al. [8] first related the minimum

* Corresponding author. Tel.: +82 10 3324 3660.
E-mail addresses: drake.yoon@gmail.com (H. Yoon), seo2h@kari.re.kr (H.H. Seo), hongtaek@kari.re.kr (H.-T. Choi).

http://dx.doi.org/10.1016/j.ast.2014.09.002
1270-9638/

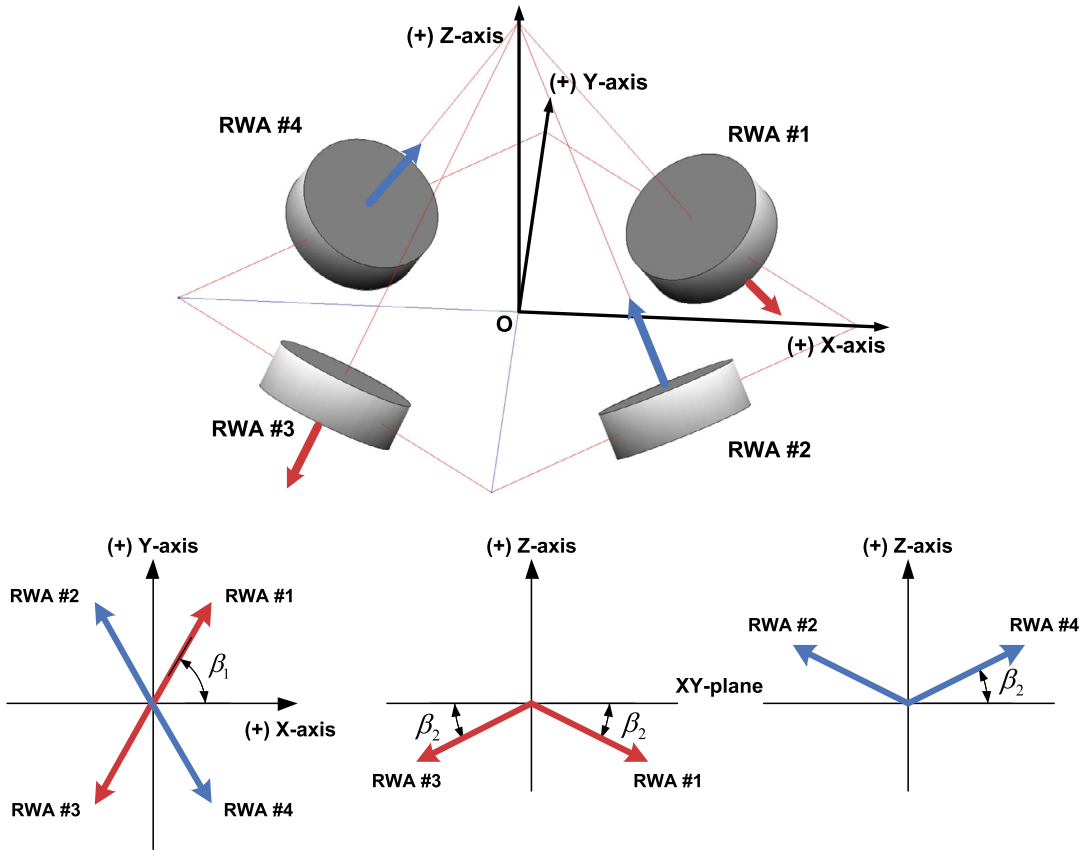

Fig. 1. Reaction wheel array in the pyramid configuration.

infinity-norm problem to spacecraft attitude control with reaction wheels, and provided the motivation for the present paper. They presented the results from a study of the nature of the torque and momentum envelopes, and provided a scheme to define them. They also proposed an attitude control loop based on their minimum infinity-norm solution algorithm. Their paper clearly revealed the geometric aspects of the envelopes, and their results are widely applicable to general configuration (e.g., in terms of number of wheels, sizes, and axis directions) of a reaction wheel array. Their method, however, is based upon a purely geometric approach without considering coding efficiency, meaning that there is room for improvement in terms of coding and computational efficiency. Verbin and Ben-Asher [9] also proposed an algorithm for a case with four reaction wheels.

In this paper, simpler and computationally more efficient methods are proposed than those presented in the earlier works [8, 9]. Our works is focused on the pyramid configuration with four identical reaction wheels, which is in fact the industry standard owing to its minimum number of redundancies and its symmetric capacities. We propose a simple new method which defines the momentum/torque envelopes. Then we provide a scheme to optimize the pyramid configuration for the inertia properties of a given spacecraft, using the relationship between its moment of inertia, and the envelope under consideration. For the distribution of the torque/momentum, we herein propose a new algorithm to obtain the minimum infinity-norm solution, that also runs much faster than that of Ref. [8].

Another distinct feature of the present work is that it provides another new algorithm which calculates an optimal momentum distribution with the wheel speeds minimally diverging from a nominal set value, in the sense of the L_∞-norm distance. This algorithm can be used to make the wheel speeds stay as close to the (non-zero) nominal speeds as possible, even when the total angular momentum of the array is zero. This feature is useful in practice to keep the wheels from operating at, or crossing zero rpm (at which wheel characteristics become nonlinear due to static and Coulomb friction). This nonlinear behavior near zero rpm may instantaneously increase the attitude control error and degrade the mechanical and electrical reliability of the wheel. So, in some space programs, it is preferable to avoid the zero rpm operation completely, if possible.

Finally, comparative numerical simulations are provided to show the effectiveness of the proposed methods. It will be shown that a control loop using the proposed methods, yields superior agility performance over the conventional L_2-norm method, and also successfully leads the wheels to a given non-zero nominal speed after completing the maneuver.

2. Momentum and torque envelope

2.1. The pyramid configuration

In this section, we propose a new means of composing the momentum and the torque envelopes of a reaction wheel array. This paper mainly deals with a four-wheel array in a pyramid configuration of the type shown in Fig. 1, which is the most common in practice. (The direction of each spin axis can be flipped, but it is defined intentionally, as shown in Fig. 1, to make the null space vector according to Eq. (4). The reason will be explained in Section 4.3.)

Let us denote the wheel spin direction vectors by $W = [\hat{w}_1, \cdots, \hat{w}_4]_{3\times 4}$; the total angular momentum $\mathbf{H}_t \in R^3$ and the angular momenta vector of the array $\mathbf{H}_w = [H_1, \cdots, H_4]^T \in R^4$ are then related according to

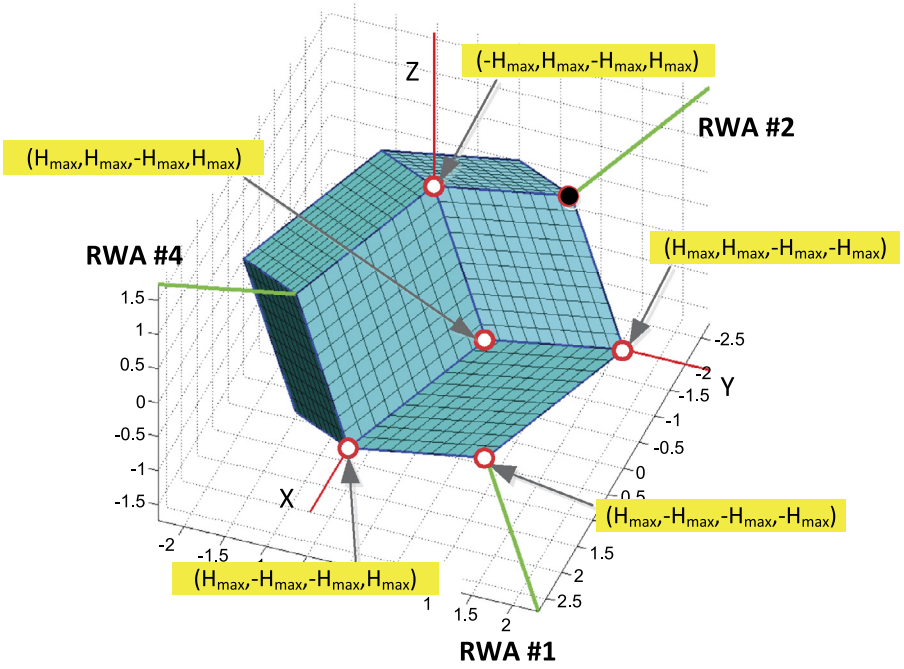

Fig. 2. Momentum envelope of a reaction wheel array in the pyramid configuration with $H_i \in [-H_{\max}, H_{\max}]$. (For interpretation of the references to color in this figure legend, the reader is referred to the web version of this article.)

$$\mathbf{H}_t = W\mathbf{H}_w, \tag{1}$$

and the torque relationship can be written as

$$\mathbf{T}_t = W\mathbf{T}_w, \tag{2}$$

where $\mathbf{T}_t \in R^3$ is the total torque and $\mathbf{T}_w = [T_1, \cdots, T_4]^T \in R^4$ is the torque vector of the wheel array. With the specific configuration shown in Fig. 1, the matrix W can be expressed as

$$W = \begin{bmatrix} \cos\beta_1\cos\beta_2 & -\cos\beta_1\cos\beta_2 & -\cos\beta_1\cos\beta_2 & \cos\beta_1\cos\beta_2 \\ \sin\beta_1\cos\beta_2 & \sin\beta_1\cos\beta_2 & -\sin\beta_1\cos\beta_2 & -\sin\beta_1\cos\beta_2 \\ -\sin\beta_2 & \sin\beta_2 & -\sin\beta_2 & \sin\beta_2 \end{bmatrix} \tag{3}$$

The momentum of each wheel H_i, where $i = 1, \cdots, 4$, is assumed to be limited as $H_i \in [-H_{\max}, H_{\max}]$, and the wheel torque T_i $(i = 1, \cdots, 4)$ as $T_i \in [-T_{\max}, T_{\max}]$. It should be noted that in the pyramid configuration, the total momentum and the total torque become zero when the four individual wheels have the same wheel momentum or torque, respectively. In other words, W has a null vector

$$\mathbf{H}_{w,n} = \alpha[1, 1, 1, 1]^T, \tag{4}$$

which yields $\mathbf{H}_t = W\mathbf{H}_{w,n} = 0$.

2.2. Momentum and torque envelopes

The momentum envelope is defined as the maximum momentum capacity of $\mathbf{H}_t$ in three-dimensional space, which can be produced by the array of reaction wheels, each with momentum constraints. (The torque envelope can be similarly defined.) Markley et al. [8] presented a detailed study of the envelope and proposed a method to visualize it, but their method is based on a geometric approach and thus may not intended to be computationally efficient. Here, a new and simpler method is presented to obtain the envelopes of the four-wheel pyramid configuration. According to earlier studies [5] and [8], the total angular momentum reaches the envelope only if at least two out of four wheels have the min/max angular momentum (i.e., $\pm H_{\max}$). In other words, the surface of the envelope consists of the locus facets of the total angular momentum with two wheel speeds saturated and the other wheel speeds set free, within their speed limits. (See also Necessary Condition 1, presented later.) This is, however, a necessary but not a sufficient condition; hence, some of the locus facets are not on the envelope surfaces, but lie inside them.

For example, let us assume that the No. 1 and 2 wheels are saturated, and that the No. 3 and 4 wheels are free. We can then obtain four locus facets,

$$(H_1, H_2) = (-H_{\max}, -H_{\max}), \qquad (H_1, H_2) = (H_{\max}, H_{\max}) \tag{5a}$$

$$(H_1, H_2) = (H_{\max}, -H_{\max}), \qquad (H_1, H_2) = (-H_{\max}, H_{\max}) \tag{5b}$$

with H_3 and H_4 being free within their limits. Among these combinations, the first two facets (with Eq. (5a)) contain the null angular momentum cases $\mathbf{H}_w = [-H_{\max}, -H_{\max}, -H_{\max}, -H_{\max}]^T$ and $\mathbf{H}_w = [H_{\max}, H_{\max}, H_{\max}, H_{\max}]^T$. This implies that these two facets are obviously not on the envelope surface. The other facets with Eq. (5b) may still be parts of the envelope surface. Therefore, we can select 12 facets $(= C(4, 2) \times 2)$ in this way, which can be obtained via

$$\begin{aligned} &(H_i, H_j) = (H_{\max}, -H_{\max}) \quad \text{and} \quad H_k \in [-H_{\max}, H_{\max}] \quad \forall k \neq i, j \\ &(H_i, H_j) = (-H_{\max}, H_{\max}) \quad \text{and} \quad H_k \in [-H_{\max}, H_{\max}] \quad \forall k \neq i, j \end{aligned} \tag{6}$$

where $i, j = 1, \cdots, 4$ and $i \neq j$. These facets actually complete the momentum envelope, as shown in Fig. 2 (red lines are spacecraft body axes, green lines are spin axes of the reaction wheels). This derivation may not seem very rigorous, but it certainly yields a correct result and is suitable for practical purposes.

3. Wheel configuration for optimal agility performance

The envelope is not a sphere but a polyhedron which can be skewed depending on the configuration of the wheel array, as shown in Fig. 2. This fact indicates that the magnitudes of the available torque/momentum may also vary in different directions.

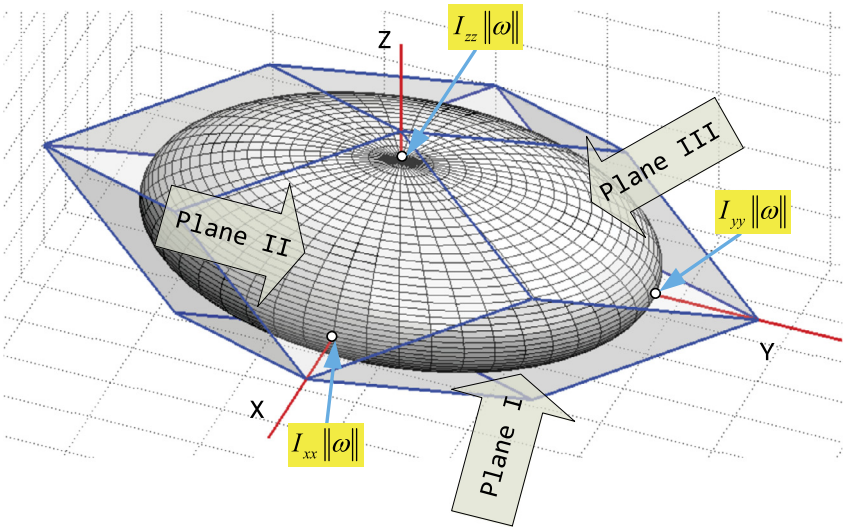

Fig. 3. Momentum envelope (blue-lined, semi-transparent) and momentum ellipsoid (gray, gridded) with the spacecraft moment of inertia $I_{xx} : I_{yy} : I_{zz} = 2 : 3 : 1$. (For interpretation of the references to color in this figure legend, the reader is referred to the web version of this article.)

In addition, spacecraft are not inertially symmetric in general, implying that the magnitudes of the available body rate and acceleration also vary along the rotational direction. Thus, in the present paper, we define the optimality of agility performance in the sense that the available body rate and the acceleration vectors along the *'worst'* direction (along which the vectors have minimum magnitude) have the largest magnitude (i.e., we define a *maximin* problem). It is also assumed that the maneuver is executed as an eigenaxis rotation in which the body rate and the acceleration vectors have a common, body-fixed direction during the maneuver. This rotation can be achieved with control logic available in the literature [10,11].

In most cases, the configuration angle β_1 is set to $\beta_1 = 45°$ for symmetry between the x and y axes. Another configuration angle β_2, which is referred to as a skew (or cant) angle, is commonly set to $\beta_2 = 35.26°$ ($\tan\beta_2 = 1/\sqrt{2}$) [8]. These values give the total torque/momentum along the spacecraft body axes the same magnitude, while also maximizing the minimum distance from the origin to the envelope surface [6,8]. This choice is made, however, without consideration of the inertia property of the spacecraft.

Another choice of configuration angles can be made with consideration of the spacecraft inertia. For simplicity, let us consider a spacecraft whose body axes are the principal axes, that is, the products of inertia are negligible and the spacecraft's matrix of inertia is $I = \mathrm{diag}([I_{xx}, I_{yy}, I_{zz}])$. This set of optimal β_1 and β_2 values can be calculated easily by equating a body rate or an acceleration, along each of the spacecraft body axes, to each other. From the following relationships

$$\omega_{x,\max} = \frac{H_{x,\max}}{I_{xx}} = \frac{4}{I_{xx}} H_{\max} \cos\beta_1 \cos\beta_2 \tag{7a}$$

$$\omega_{y,\max} = \frac{H_{y,\max}}{I_{yy}} = \frac{4}{I_{yy}} H_{\max} \sin\beta_1 \cos\beta_2 \tag{7b}$$

$$\omega_{z,\max} = \frac{H_{z,\max}}{I_{zz}} = \frac{4}{I_{zz}} H_{\max} \sin\beta_2 \tag{7c}$$

and

$$\omega_{x,\max} = \omega_{y,\max} = \omega_{z,\max}, \tag{8}$$

where $H_{\bullet,\max}$, $(\bullet = x, y, z)$ is the maximum total momentum along the spacecraft body axes, the optimal configuration angles β_1 and β_2 can be obtained as

$$\tan\beta_1 = \frac{I_{yy}}{I_{xx}} \tag{9a}$$

$$\tan\beta_2 = \frac{I_{zz}}{\sqrt{I_{xx}^2 + I_{yy}^2}}, \tag{9b}$$

and the maximum momentum along each body axis is

$$\omega_{x,\max} = \omega_{y,\max} = \omega_{z,\max} = \frac{4H_{\max}}{\sqrt{I_{xx}^2 + I_{yy}^2 + I_{zz}^2}}. \tag{10}$$

Here, it should be noted that the maximum slew rates in Eq. (10) cannot be obtained simultaneously; instead, each of them is obtained when the total momentum is aligned along the corresponding body axis.

The above-mentioned method is very convenient; however, as far as the authors are aware, it has yet to be proved that Eq. (9) is actually the optimal solution which yields the maximum worst body rate. Here, we present a discussion of the optimality by introducing a *momentum ellipsoid* and its relationship with the momentum envelope. The momentum ellipsoid is defined as the locus of the angular momentum vector required for the spacecraft to have an angular rate with a given magnitude $\|\omega\|$. The ellipsoid has a shape which is obviously determined by the spacecraft inertial property, and is scaled by the given value of $\|\omega\|$. The ellipsoid has three semi-axes along the spacecraft body axes, and each length is proportional to the principal moment of inertia (I_{ii}) about each body axis, and the corresponding slew rate $\|\omega\|$, as shown in Fig. 3. In rectangular coordinates, the equation of the ellipsoid is:

$$\frac{x^2}{I_{xx}^2} + \frac{y^2}{I_{yy}^2} + \frac{z^2}{I_{zz}^2} = \|\omega\|^2. \tag{11}$$

To maximize the available slew rate $\|\omega\|$ along the worst rotational direction, we need to find the optimal configuration of the wheel array such that the momentum ellipsoid inscribed in the momentum envelope, has a maximum value of $\|\omega\|$. Due to symmetry, only the three facets of the envelope which make tangential contact with the ellipsoid should be considered. From some geometric relationships and calculations, it can be shown that the magnitude of the spacecraft slew rates, which put the ellipsoid tangentially into contact with Planes I, II, and III (see Fig. 3) are:

$$\omega_{\mathrm{I}}^2 = \frac{16\sin^2\beta_1\cos^2\beta_1\cos^2\beta_2}{I_{xx}^2\sin^2\beta_1 + I_{yy}^2\cos^2\beta_1} \tag{12a}$$

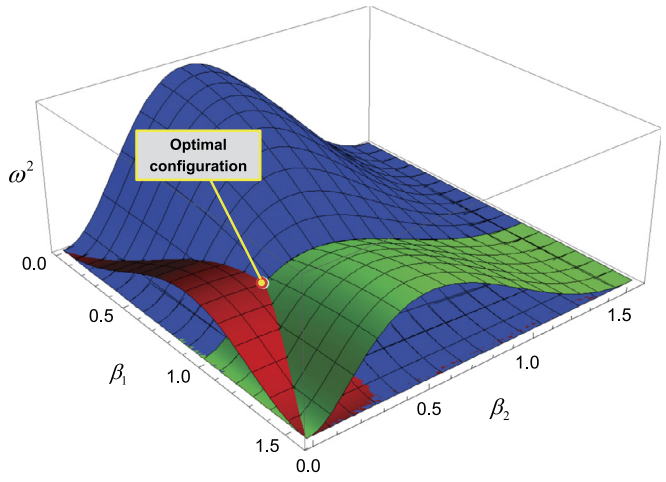

Fig. 4. Square of the slew rates ω_{I} (red), ω_{II} (blue), and ω_{III} (green) and the optimal configuration. (For interpretation of the references to color in this figure legend, the reader is referred to the web version of this article.)

$$\omega_{\mathrm{II}}^2 = \frac{16\cos^2\beta_1 \sin^2\beta_2 \cos^2\beta_2}{I_{xx}^2 \sin^2\beta_2 + I_{zz}^2 \cos^2\beta_1 \cos^2\beta_2} \tag{12b}$$

$$\omega_{\mathrm{III}}^2 = \frac{16\sin^2\beta_1 \sin^2\beta_2 \cos^2\beta_2}{I_{yy}^2 \sin^2\beta_2 + I_{zz}^2 \sin^2\beta_1 \cos^2\beta_2} \tag{12c}$$

respectively. Next, we can obtain the optimal configuration angles which *maximize* the *minimum* among ω_{I}, ω_{II}, and ω_{III}. Fig. 4 shows the square of the slew rates versus the configuration angles using Eq. (12). It can be shown that the optimal configuration angles can be obtained when $\omega_{\mathrm{I}}^2 = \omega_{\mathrm{II}}^2 = \omega_{\mathrm{III}}^2$. In other words, the optimal configuration can be obtained when the momentum ellipsoid simultaneously comes into contact with all the facets of the envelope. From Eqs. (12) and this condition, one can obtain Eq. (9).

There are twelve worst directions in total, along which the maximum available body rate is minimized. They are parallel with the following vectors:

$$[\pm I_{xx}, \pm I_{yy}, 0]^T, \tag{13a}$$

$$[\pm I_{xx}, 0, \pm I_{zz}]^T, \tag{13b}$$

$$[0, \pm I_{yy}, \pm I_{zz}]^T. \tag{13c}$$

The maximum worst body rate with the optimal configuration can also be expressed as

$$\omega_{\mathrm{I}} = \omega_{\mathrm{II}} = \omega_{\mathrm{III}} = \frac{2\sqrt{2}H_{\max}}{\sqrt{I_{xx}^2 + I_{yy}^2 + I_{zz}^2}}, \tag{14}$$

which is only $1/\sqrt{2}$ (≈ 70 %) of the maximum body rate along the body axes in Eq. (10).

Note that the conventional choice of configuration angles (i.e., $\beta_1 = 45^\circ$ and $\tan\beta_2 = 1/\sqrt{2}$) is optimal only when the spacecraft is inertially symmetric (i.e., when $I_{xx} = I_{yy} = I_{zz}$).

4. Optimal torque/momentum distribution

The aforementioned optimal configuration would not be of much use, unless the attitude control law fully utilizes its optimized capacities. Therefore, such an attitude control law should be employed to achieve optimal agility performance.

An attitude control law calculates the attitude error and then calculates the required torque and/or the momentum command in the three-dimensional body frame. A command distribution logic is then used to calculate the distribution of the three-dimensional commands to the individual reaction wheels. In this section, we present new algorithms for the optimal torque/momentum distribution.

4.1. The minimum L_2-norm (or conventional) method

The most commonly used solution in practice is the minimum L_2-norm solution, which is given by

$$\mathbf{T}_{w,2} = W^+ \mathbf{T}_t \tag{15}$$

where W^+ is the pseudo-inverse matrix. The L_2-norm is defined as the sum of the squares of the individual elements, i.e., $\|\mathbf{x}\|_2 = \sqrt{x_1^2 + x_2^2 + \cdots + x_N^2} = \sqrt{\mathbf{x}^T\mathbf{x}}$, for a vector $\mathbf{x} = [x_1, \cdots, x_N]^T$. Because the L_2-norm can be interpreted as the total energy or power of the vector signal, this method yields optimal power-efficiency. However, for the power efficiency, this method allocates as large a command as possible to a wheel whose spin axis is closest to the total commanded torque/momentum. This leads the wheel to be easily saturated even when the total torque/momentum does not reach the envelopes yet. Therefore, it can be concluded that this method does not fully utilize the capacities of the wheel array, and is thus not optimal in terms of agility performance.

4.2. The minimum L_∞-norm method

Because each wheel has limited torque/momentum capacities, the total angular momentum and the torque are also constrained within the envelopes. Therefore, optimal maneuvering performance can be accomplished by delaying wheel speed saturation as much as possible. This can be achieved by minimizing the maximum value, or L_∞-norm, of the set of individual wheel momentum/torque values [8]. The L_∞-norm of a vector $\mathbf{x} = [x_1, \cdots, x_N]^T$ is defined as

$$\|\mathbf{x}\|_\infty = \max\big(|x_1|, |x_2|, \cdots, |x_N|\big). \tag{16}$$

The minimum L_∞-norm method enables the wheel array to fully utilize its torque/momentum capacities. Unlike the minimum L_2-norm solution, the minimum L_∞-norm solution cannot be expressed in a simple closed-form. Therefore, a sophisticated algorithm which *searches* for the solution is necessary. Markley et al. [8] presented such an algorithm based on the geometric properties of the solution.

4.3. New algorithm for the minimum L_∞-norm solution

In this section, a new, computationally efficient algorithm is proposed to find the minimum L_∞-norm solution. For a given under-determined linear equation (2), all of the solutions can be written in a general form as

$$\mathbf{T}_w = \mathbf{T}_{w,2} + \mathbf{T}_{\mathrm{null}} \tag{17}$$

where $\mathbf{T}_{w,2} = W^+\mathbf{T}_t$ is the minimum L_2-norm solution and $\mathbf{T}_{\mathrm{null}}$ is the null vector of the matrix W, which satisfies $W\mathbf{T}_{\mathrm{null}} = 0$.

At this point, a case is considered in which there are four wheels and the nullity of W is 1. (The wheel sizes and the spin directions may not be symmetric at this point.) The null vector $\mathbf{T}_{\mathrm{null}}$ can be expressed as

$$\mathbf{T}_{\mathrm{null}} = \alpha[T_{n,1}, T_{n,2}, T_{n,3}, T_{n,4}]^T \tag{18}$$

where α is any real scalar number and where the vector $[T_{n,1}, T_{n,2}, T_{n,3}, T_{n,4}]^T$ is the basis of the null space of W. Note that $T_{n,i} \neq 0$ $(i = 1, \cdots, 4)$ when any combination of three column vectors (or the spin axes) of W spans a three-dimensional

space, which is true for the pyramid configuration. This can easily be proved by showing that the assumption of $T_{n,j} = 0$ for any j yields $T_{n,i} = 0$, $\forall i$. The general form of the solution, Eq. (17), can then be written as

$$\begin{bmatrix} T_1 \\ T_2 \\ T_3 \\ T_4 \end{bmatrix} = \begin{bmatrix} T_{2,1} \\ T_{2,2} \\ T_{2,3} \\ T_{2,4} \end{bmatrix} + \begin{bmatrix} \alpha T_{n,1} \\ \alpha T_{n,2} \\ \alpha T_{n,3} \\ \alpha T_{n,4} \end{bmatrix}. \tag{19}$$

At this point, we will use some necessary conditions for the minimum L_∞-norm solution to derive the problem solving algorithm. The first is well known and is given as follows.

Necessary Condition 1. *At least two elements of the minimum L_∞-norm solution have the same absolute value as the L_∞-norm of the solution itself. (Of course, the absolute value of these elements is greater than, or equal to, the others.)*

Proof. The proof is omitted (see Refs. [5,8]). □

Necessary Condition 1 is closely related to the fact that at least two wheels are saturated at the momentum envelope, as shown in the previous section. Before introducing the second condition, we make an assumption to simplify the derivation process.

Assumption 1. *All of the elements of the null space basis, $T_{n,i}$, ($i = 1, \cdots, 4$) have the same sign (e.g., positive), such that $T_{n,i} > 0$.*

This assumption does not lose any generality; one can flip the sign of any $T_{n,i}$ by flipping the direction of $\hat{w}_i$. Note that the spin directions defined in Fig. 1 satisfy this assumption. The second necessary condition is presented below.

Necessary Condition 2. *All of the elements in Necessary Condition 1 (whose absolute values are identical to the L_∞-norm), do not have the same sign.*

Proof. Let $\mathbf{T}$ be the minimum L_∞-norm solution and assume that its elements, of which the absolute values are identical to the minimum L_∞-norm, have a same sign. Then, because the elements of the null basis vector, $T_{n,i}$, also have a same sign (from Assumption 1), there always exists a null vector $\mathbf{T}_{\text{null}}$ which gives the solution $\mathbf{T} + \mathbf{T}_{\text{null}}$, a smaller L_∞-norm. This violates the assumption that $\mathbf{T}$ is the minimum L_∞-norm solution. □

From these necessary conditions, an algorithm can be derived to calculate the solution. There are six ($= C(4,2)$) possible candidates of α which may make $\mathbf{T}_w$ the solution, as follows:

$$\begin{aligned}
\alpha &= -\tfrac{T_{2,1}+T_{2,2}}{T_{n,1}+T_{n,2}} \quad \leftrightarrow \quad \langle 1,2 \rangle, \\
\alpha &= -\tfrac{T_{2,1}+T_{2,3}}{T_{n,1}+T_{n,3}} \quad \leftrightarrow \quad \langle 1,3 \rangle, \\
\alpha &= -\tfrac{T_{2,1}+T_{2,4}}{T_{n,1}+T_{n,4}} \quad \leftrightarrow \quad \langle 1,4 \rangle, \\
\alpha &= -\tfrac{T_{2,2}+T_{2,3}}{T_{n,2}+T_{n,3}} \quad \leftrightarrow \quad \langle 2,3 \rangle, \\
\alpha &= -\tfrac{T_{2,2}+T_{2,4}}{T_{n,2}+T_{n,4}} \quad \leftrightarrow \quad \langle 2,4 \rangle, \\
\alpha &= -\tfrac{T_{2,3}+T_{2,4}}{T_{n,3}+T_{n,4}} \quad \leftrightarrow \quad \langle 3,4 \rangle.
\end{aligned} \tag{20}$$

In these equations, $\langle p, q \rangle$ indicates that the corresponding value of α is derived from the condition that the p-th and the q-th elements have the same absolute value but have different signs. For example, the first condition comes from $T_{2,1} + \alpha T_{n,1} = -(T_{2,2} + \alpha T_{n,2})$. Then, the minimum L_∞-norm solution can be obtained by comparing the maximum absolute values of the elements of the general solution in Eq. (19) with the six candidates of α, as given in Eq. (20), and then selecting the one with the lowest value. The newly developed algorithm can be implemented with far fewer code lines and can run much faster (typically more than five times faster with MATLAB) than the previous method proposed by Markley et al. [8].

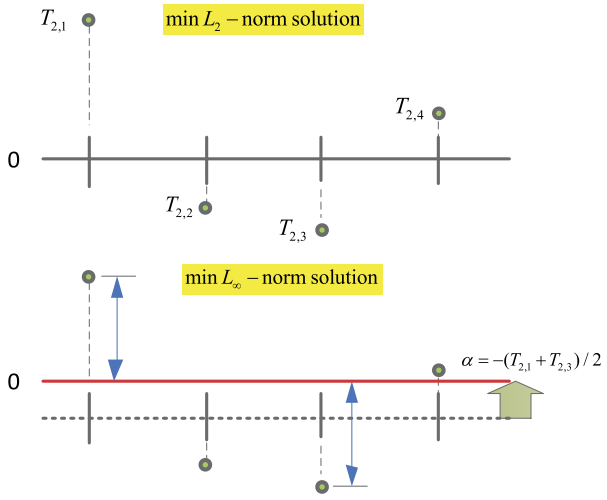

Fig. 5. Minimum L_2-norm (top) and minimum L_∞-norm (bottom) solutions in the pyramid configuration.

4.4. A special case: the symmetric pyramid configuration

For the symmetric pyramid configuration, described in Section 2.1, for which the wheels are identical and spin axes are symmetric (as shown in Fig. 1), the null basis vector can be written as $[1, 1, 1, 1]^T$. From the symmetry of this configuration, an even simpler algorithm can be derived.

Let us assume that the minimum L_2-norm solution, $\mathbf{T}_{w,2}$, is calculated as shown at the top of Fig. 5. Because the null vector can be written as $\mathbf{T}_{\text{null}} = \alpha[1, 1, 1, 1]^T$, the addition of this null vector $\mathbf{T}_{\text{null}}$ to $\mathbf{T}_{w,2}$ can be geometrically interpreted as a shift of the solution with α, or an equivalent shift of the 'zero'-line with $-\alpha$. Therefore, it can be intuitively concluded that the minimum L_∞-norm solution, $\mathbf{T}_{w,\infty}$, can be obtained as

$$\mathbf{T}_{w,\infty} = \mathbf{T}_{w,2} + \alpha[1, 1, 1, 1]^T \tag{21}$$

where $-\alpha$ is the average of the min/max values of $\mathbf{T}_{w,2}$; that is,

$$\alpha = -\frac{\min(\mathbf{T}_{w,2}) + \max(\mathbf{T}_{w,2})}{2} \tag{22}$$

where $\min(\cdot)$ and $\max(\cdot)$ are the minimum and the maximum values of the elements, respectively. Owing to the symmetry of the pyramid configuration, the solution can be obtained without comparing the norms of the multiple candidates (as in the previous section). This algorithm can easily be implemented by adding only few code lines to the conventional L_2-norm method. For the symmetric pyramid configuration, the minimum L_∞-norm solution probably cannot be simpler than the newly proposed one.

4.5. Minimum L_∞-distance solution from nominal values

The wheel momentum distribution using the minimum L_∞-norm solution can be successfully used for slew maneuver control. However, this method will make the speed of each individual wheel zero when the total angular momentum command is zero, because this state obviously has the minimum L_∞-norm value.

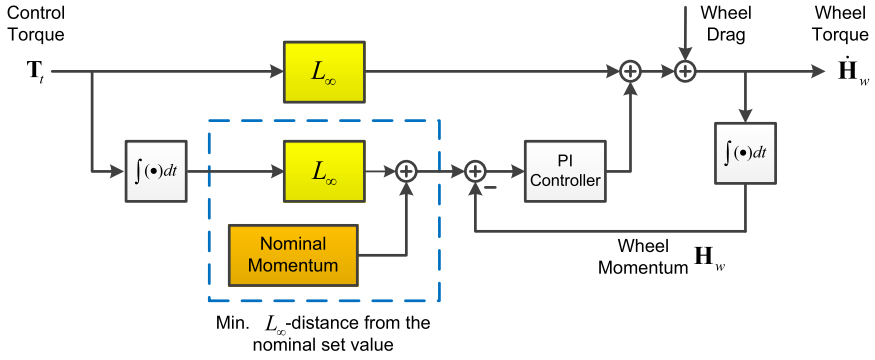

Fig. 6. Combined torque and modified momentum control loops.

Thus, if a spacecraft has zero-bias momentum, the wheel speeds become zero when the spacecraft completes a maneuver and is at rest. As noted in the introduction, it is not preferable for a reaction wheel to operate near zero rpm due to its nonlinear behavior. This behavior can cause considerable attitude errors, and thus may hinder performance of assigned tasks. Moreover, if the wheels are kept in low rpm range for long, there might be some impact on wheel reliability. (For this reason, some wheel manufacturers set limits on the allowable number of turns at low rpm.)

The present section proposes a new algorithm with which the wheel speed vector has the minimum L_∞-distance from a given (non-zero) nominal speed. This algorithm can be derived in a manner similar to that in Section 4.3. It can easily be shown that the solution with minimum $\mathcal{L}_\infty$-distance from a nominal vector, $\mathbf{H}_{\text{nom}} = [\bar{H}_1, \bar{H}_2, \bar{H}_3, \bar{H}_4]^T$, has at least two elements which have the same absolute difference from the nominal momentum elements, and this absolute difference is greater than, or equal to, those of the other elements. Hence, we can have six possible candidates of α as below.

$$\begin{aligned}
\alpha &= -\frac{(H_{2,1}+H_{2,2})-(\bar{H}_1+\bar{H}_2)}{H_{n,1}+H_{n,2}} \quad \leftrightarrow \quad \langle 1,2\rangle \\
\alpha &= -\frac{(H_{2,1}+H_{2,3})-(\bar{H}_1+\bar{H}_3)}{H_{n,1}+H_{n,3}} \quad \leftrightarrow \quad \langle 1,3\rangle \\
\alpha &= -\frac{(H_{2,1}+H_{2,4})-(\bar{H}_1+\bar{H}_4)}{H_{n,1}+H_{n,4}} \quad \leftrightarrow \quad \langle 1,4\rangle \\
\alpha &= -\frac{(H_{2,2}+H_{2,3})-(\bar{H}_2+\bar{H}_3)}{H_{n,2}+H_{n,3}} \quad \leftrightarrow \quad \langle 2,3\rangle \\
\alpha &= -\frac{(H_{2,2}+H_{2,4})-(\bar{H}_2+\bar{H}_4)}{H_{n,2}+H_{n,4}} \quad \leftrightarrow \quad \langle 2,4\rangle \\
\alpha &= -\frac{(H_{2,3}+H_{2,4})-(\bar{H}_3+\bar{H}_4)}{H_{n,3}+H_{n,4}} \quad \leftrightarrow \quad \langle 3,4\rangle
\end{aligned} \tag{23}$$

where $H_{n,i}$ $(i = 1, \cdots, 4)$ are the elements of the null vector of W. Then we can choose α which makes the solution have the minimum $\mathcal{L}_\infty$-distance from $\mathbf{H}_{\text{nom}}$.

If the null basis vector is $[1, 1, 1, 1]^T$ (as in the symmetric pyramid configuration), and if the nominal wheel momentum of each wheel also has the same value (for instance H_{nom}), it becomes possible to obtain the solution more easily. Because the nominal wheel momentum vector $\mathbf{H}_{\text{nom}} = H_{\text{nom}}[1, 1, 1, 1]^T$ is itself a null vector of W, the sum of this vector and the minimum L_∞-norm solution $\mathbf{H}_{w,\infty}$, that is,

$$\mathbf{H}^n_{w,\infty} = \mathbf{H}_{w,\infty} + \mathbf{H}_{\text{nom}}, \tag{24}$$

also becomes a solution for Eq. (1). Moreover, because $\mathbf{H}_{w,\infty}$ has the minimum L_∞-distance from the zero vector $[0, 0, 0, 0]$, the solution $\mathbf{H}^n_{w,\infty}$ has the minimum L_∞-distance from the nominal momentum vector $H_{\text{nom}}[1, 1, 1, 1]^T$, and thus is the minimum L_∞-distance solution. It is noticeable that the solution Eq. (24) also can be obtained from Eq. (23) with $H_{n,i} = 1$ and $\bar{H}_i = H_{\text{nom}}$ for $\forall i$ and a proper choice of α.

Fig. 6 shows the attitude control loop, which consists of the minimum L_∞-norm torque distribution and the modified minimum L_∞-distance momentum distribution with respect to the nominal speed. Its structure is nearly identical to that of Ref. [8] except for the use of the modified minimum L_∞-distance momentum distribution. Using this control loop, it is now possible to lead the wheel speeds to the (non-zero) nominal set value when the spacecraft is at rest.

It should be noted that this method (especially with a large nominal set value) may cause the wheels to become saturated easily and thus may hinder optimal use of the full momentum capacity. Therefore, the nominal value should be selected with great care: it should not be too large (reduction of the available momentum capacity) or too small (attitude control performance at rest and degraded reliability of the wheels). One may use a variable nominal value, which is zero when the total momentum is large (to fully utilize the momentum capacity) and is sufficiently large when the total momentum is small (to keep the wheel speeds away from zero rpm).

In some actual space programs, for instance, those involving imaging satellites, interruption of an imaging mission due to wheel speed zero-crossing should be avoided. In addition, it may be a case that reliability of the wheels has higher priority than agility performance. For such cases, one may force the wheels to operate only within the half of the speed range without a sign change, that is, with $H_i \in [0, H_{\max}]$. This scheme can be implemented by setting the nominal speed to half the maximum speed, and setting saturation limits at zero and the maximum rpm. Of course, as the momentum envelope is reduced to half the original one, some agility performance should be sacrificed. However, the torque capacity remains the same, and it is also a dominant factor for agility performance, especially in small angle slews, so the sacrifice of agility performance may not be that great, and may be tolerable depending on the mission requirements.

5. Numerical simulation

Comparative simulation examples are given in this section. The spacecraft inertia property is $I = \text{diag}[I_{xx}, I_{yy}, I_{zz}] = \text{diag}[1000, 1500, 500]$ kg m^2, and for each reaction wheel, the inertia is 0.4 kg m^2. The maximum wheel torque is 2 Nm, and the maximum wheel speed is 600 rpm. (These values are roughly based on actual satellites developed and operated by Korea Aerospace Research Institute.) It is assumed that the spacecraft is initially at rest and that the total angular momentum of the wheel array is initially zero (i.e., zero-momentum bias). The spacecraft is assumed to be commanded to perform a slew maneuver of 60 deg. The rotational axis is set to $-I^{-1}\hat{w}_2$, where $\hat{w}_2$ is the spin axis of Wheel #2, so that the required total angular momentum vector is aligned with $\hat{w}_2$. This choice will distinctly show the difference between the conventional L_2-norm method and the newly

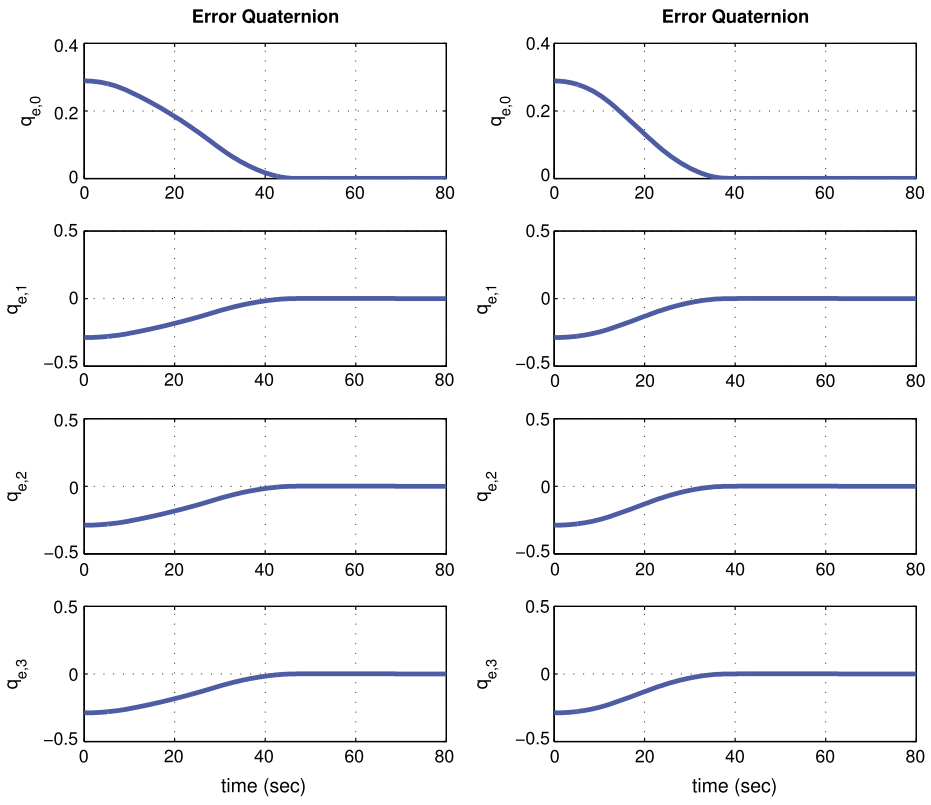

(a) L_2-method (b) L_∞-method

Fig. 7. Attitude error quaternions.

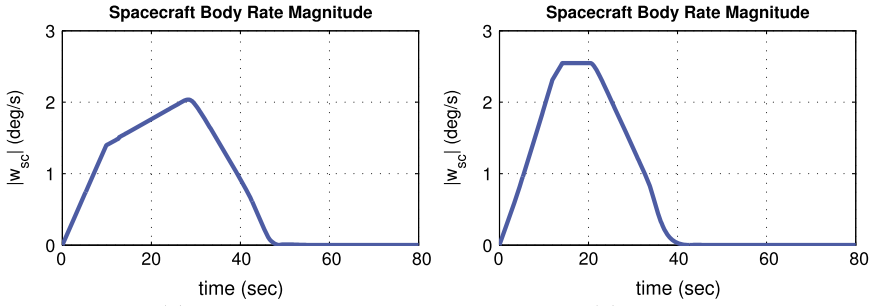

(a) L_2-method (b) L_∞-method

Fig. 8. Spacecraft body rate magnitude.

proposed L_∞-norm method (will be shown later). For the given inertial property, the optimal configuration angles are computed to be $\beta_1 = 56.3°$ and $\beta_2 = 15.5°$ using Eq. (9). These values are used during the comparison of the performance of the L_2-norm and the L_∞-norm methods. For the attitude feedback loop, we developed a PD-control algorithm which leads the spacecraft to rotate about a fixed Euler rotational axis without excessive transient overshoot. This is a modification of an earlier scheme proposed in Ref. [10]. When using the minimum L_∞-distance control (from the nominal set value) presented in Section 4.5, the nominal speed is set to 100 rpm when the total momentum magnitude is smaller than half of the maximum momentum of one wheel; otherwise, it is set to zero rpm. During the simulation, the individual wheel torque is forced to be zero if the wheel speed is saturated (with a 30 rpm margin for practical reasons) and the commanded torque is outward the limit. This scheme keeps the wheel speeds within their allowable speed range.

Figs. 7 and 8 show the improved agility performance of the newly developed L_∞-norm method over the conventional L_2-norm method. The maneuver time (in which all of the attitude errors in each body axis become less than 0.01°) is shortened from 52 to 41 sec (reduction of about 21%) in this specific scenario, by the proposed method. More specifically, the maximum body rate was increased from 2.0 to 2.5 deg/sec, and the acceleration from 0.14 and 0.4 (before and after the saturation of Wheel #2 at 10 sec, respectively) to 0.19 deg/sec^2. These results show that the proposed method successfully improved agility performance by more fully utilizing the momentum and torque capacities.

The superiority of the proposed method is more clearly understood in Figs. 9 and 10. These display the different histories of reaction wheel speeds and the trajectory of the total angular momentum in the three-dimensional space, respectively. With both methods, the wheel speeds, which are initially at the nominal speed of 100 rpm, are operated within the given speed limits ($-600 \sim +600$ rpm). However, with the conventional L_2-norm method, Wheel #2 becomes saturated early, while the other wheels are still far from the speed limit. This occurs because

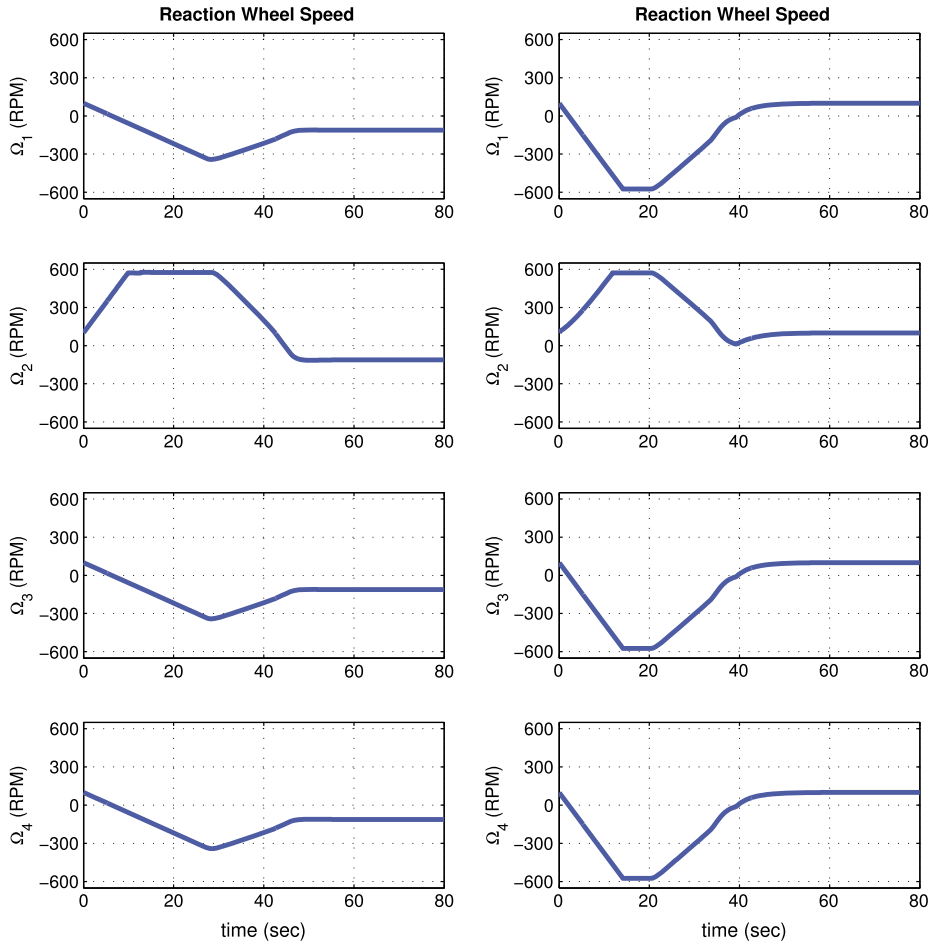

Fig. 9. Reaction wheel speeds.

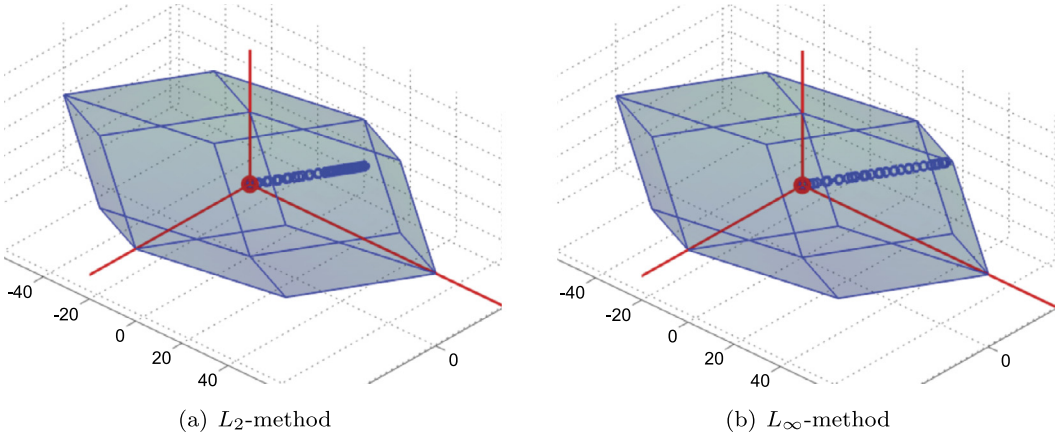

Fig. 10. Angular momentum trajectories.

the required momentum is along the axis of Wheel #2 and thus the minimum L_2-norm method uses this wheel as much as possible. After Wheel #2 is saturated, angular acceleration is decreased significantly, as shown in Fig. 8(a). On account of the reduced acceleration, the total angular momentum could not reach the envelope and return to zero, as shown in Fig. 10, to complete the 60-degree maneuver. This implies that the control law did not fully utilize the momentum capacity. Moreover, because a sort of 'symmetry' is broken when the Wheel #2 becomes saturated, the wheel speeds do not return to nominal (100 rpm) after the maneuver (see the wheel speeds after stabilization in Fig. 9(a)). The wheel speeds may converge to an unpredictable value after each maneuver, and thus may become too large or too small after a number of maneuvers. Therefore, additional operations and/or control logics may be needed to return the speeds to nominal value after maneuvers.

On the other hand, the minimum L_∞-norm method delays wheel speed saturation until the total momentum reaches the envelope so that the spacecraft can maneuver with a larger body rate. It is noteworthy that, because the required total momentum

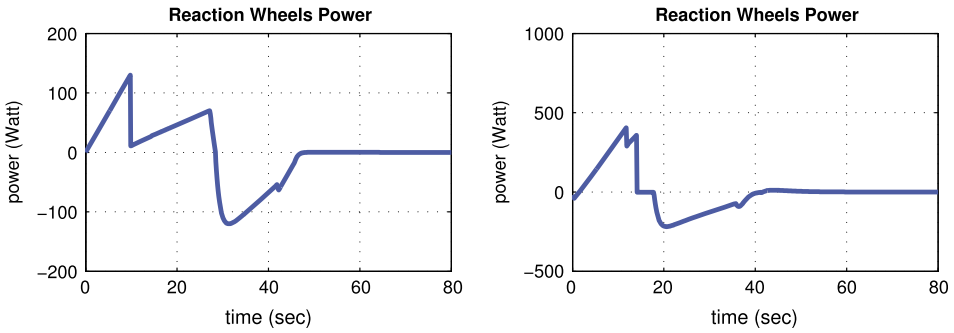

(a) L_2-method (b) L_∞-method

Fig. 11. Total power of reaction wheel array.

is along $\hat{w}_2$ in this scenario, all of the wheels are used uniformly to generate this momentum. (Note that all of the wheels should be saturated at the vertex (the black dot in Fig. 2) which lies on $\hat{w}_2$.) As shown in Fig. 10(b), the total momentum reached the envelope, which implies that the proposed method fully utilized the momentum capacity of the array. It also can be observed that the wheel speeds returned to nominal after the maneuver, owing to the minimum L_∞-distance momentum distribution scheme.

Fig. 11 shows the time histories of the total power of the wheel array. As anticipated in the discussions in Introduction and Section 4.1, the proposed L_∞-norm method shows lower power efficiency than the conventional L_2-norm method, as the cost for its superior agility performance. However, energy consumption for attitude maneuvers takes only a small portion of the total energy budget, because the time duration of maneuvers is very short compared to the whole flight time. Therefore, the lower power efficiency is generally tolerable in practice.

Finally, we conducted another simulation in which the wheel speed zero-crossing condition would be absolutely avoided. These results are shown in Fig. 12. In Fig. 12(b), it can be seen that the wheel speeds, which were initially set to a (fixed) nominal value of 300 rpm (half the maximum rpm), did not cross the zero-rpm point, and operated between 0 and +600 rpm, later returning to the initial value. The momentum capacity, and thus the maximum body rate (about 1.2 deg/sec), are each only half the original ones, but the maneuver time was 59 sec, an increase of 41%. This increase may be acceptable in some space programs, in return for better attitude pointing stability and wheel reliability.

6. Conclusions

To make the best use of a reaction wheel array, we combined geometric, mathematical, and algorithmic approaches. These methods were developed with an emphasis on computational efficiency and ease of implementation, and are therefore preferable for practical applications. The newly developed methods yield results identical to those of Markley et al. but can be implemented much easier and run faster. In addition, we proposed a new method which allows the wheels to operate as close to their nominal speed as possible. We also successfully demonstrated the validity and effectiveness of all the methods introduced here using numerical simulations.

The developed methods are applicable to a case with four reaction wheels, especially in the pyramid configuration. Therefore, extending the proposed algorithms for use with more general configurations would be worthy of further study. The authors also hope that this work promotes studies and applications of the minimum infinity-norm methods in applications other than agile maneuver. For instance, the developed methods could be applied to determine the wheel specification requirements. It could also be applied in design of the momentum management logic required

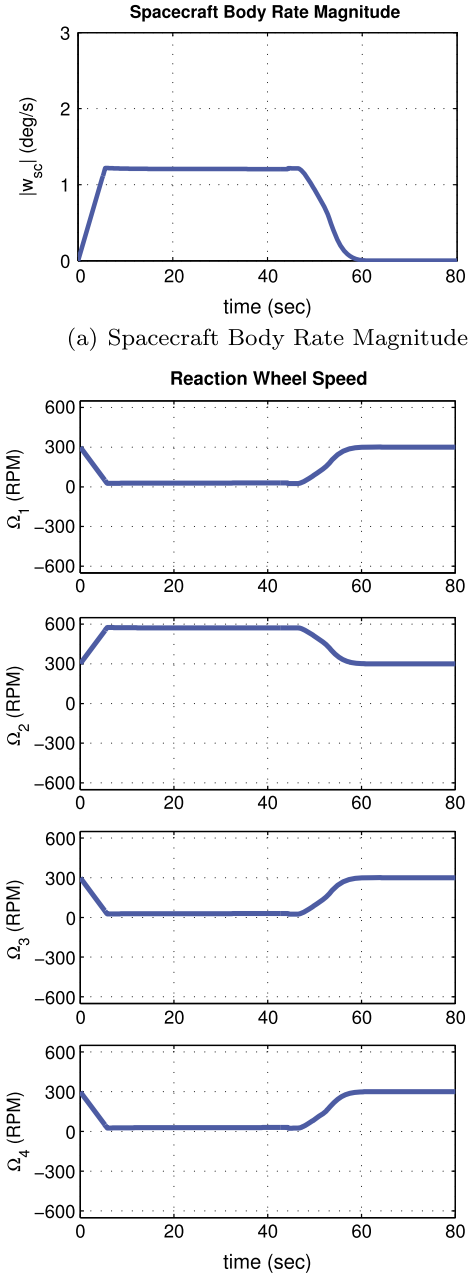

(a) Spacecraft Body Rate Magnitude

(b) Reaction Wheel Speeds

Fig. 12. Maneuver without wheel speed zero-crossing.

to compensate for external disturbances (e.g., solar pressure or air drag) applied to spacecraft. Finally, it should be mentioned that the agility performance also depends on the design of the attitude feedback control. So optimal attitude feedback design should be considered for even better agility performance, along with the methods presented in this work.

Conflict of interest statement

None declared.

References

[1] J.A. Cadzow, A finite algorithm for the minimum l_∞ solution to a system of consistent linear equations, SIAM J. Numer. Anal. 10 (4) (1973) 607–617.
[2] J.A. Cadzow, An efficient algorithmic procedure for obtaining a minimum L_-norm solution to a system of consistent linear equations, SIAM J. Numer. Anal. 11 (6) (1974) 1151–1165.
[3] Y. Choi, H. Bang, H. Lee, Dynamic control allocation for shaping spacecraft attitude control command, in: AIAA Guidance, Navigation, and Control Conference and Exhibit, 2006, pp. 21–24, AIAA 2006-6040.
[4] I.A. Gravagne, I.D. Walker, On the structure of minimum effort solutions with application to kinematic redundancy resolution, IEEE Trans. Robot. Autom. 16 (6) (2000) 855–863.
[5] I. Ha, J. Lee, A new algorithm for a minimum infinity-norm solution and its application to trajectory planning of kinematically redundant manipulators, in: 2001 IEEE/ASME International Conference on Advanced Intelligent Mechatronics, 2001. Proceedings, IEEE, 2001, pp. 446–451.
[6] H.B. Hablani, Sun-tracking commands and reaction wheel sizing with configuration optimization, J. Guid. Control Dyn. 17 (4) (1994) 805–814.
[7] O. Härkegård, Dynamic control allocation using constrained quadratic programming, J. Guid. Control Dyn. 27 (6) (2004) 1028–1034.
[8] F.L. Markley, R.G. Reynolds, F.X. Liu, K.L. Lebsock, Maximum torque and momentum envelopes for reaction-wheel arrays, J. Guid. Control Dyn. 33 (5) (2010) 1606–1614.
[9] D. Verbin, J.Z. Ben-Asher, Time efficient closed loop steering laws for rigid satellite large rotational maneuver, in: AIAA Guidance, Navigation, and Control Conference and Exhibit, 2006, pp. 1–25, AIAA 2006-6042.
[10] B. Wie, J. Lu, Feedback control logic for spacecraft eigenaxis rotations under slew rate and control constraints, J. Guid. Control Dyn. 18 (6) (1995) 1372–1379.
[11] B. Wie, D. Bailey, C. Heiberg, Rapid multitarget acquisition and pointing control of agile spacecraft, J. Guid. Control Dyn. 25 (1) (2002) 96–104.